The response of the regional longwave radiation balance and climate system in Europe to an idealized afforestation experiment

Marcus Breil[1,2], Felix Krawczyk[2], Joaquim G. Pinto[2]

[1]Institute of Physics and Meteorology, University of Hohenheim, Stuttgart, Germany

[2]Institute for Meteorology and Climate Research, Karlsruhe Institute of Technology, Karlsruhe, Germany

Correspondence to: Marcus Breil (marcus.breil@uni-hohenheim.de)

Abstract

Afforestation is an important mitigation strategy to climate change due to its carbon sequestration potential. Besides this favorable biogeochemical effect on global CO_2 concentrations, afforestation also affects the regional climate by changing the biogeophysical land surface characteristics. In this study, we investigate the effects of an idealized global CO_2 reduction to pre-industrial conditions by a Europe-wide afforestation experiment on the regional longwave radiation balance, starting in the year 1986 from a continent entirely covered with grassland. Results show that the impact of biogeophysical processes on the surface temperatures is much stronger than of biogechemical processes. Furthermore, biogeophysically induced changes of the surface temperatures, atmospheric temperatures and moisture concentrations are as important for the regional longwave radiation balance as the global CO_2 reduction. While the outgoing longwave radiation is increased in winter, it is reduced in summer. On annual total, a Europe-wide afforestation has a regional warming effect, despite reduced CO_2 concentrations. Thus, even for an idealized reduction of the global CO_2 concentrations to pre-industrial levels, the European climate response to afforestation would still be dominated by its biogeophysical effects.

1. Introduction

A highly debated strategy to achieve the Paris climate targets is afforestation (Harper et al., 2018; Roe et al., 2019). During their growth period, forests remove CO_2 from the atmosphere and store the carbon in their biomass (Luyssaert, et al., 2010; Pan et al., 2011). CO_2 concentrations in the atmosphere are consequently reduced, resulting in a reduction of the downwelling longwave radiation (DLR) and an increase of the outgoing longwave radiation at the top of the atmosphere (OLR). In this way, afforestation actively reduces the greenhouse effect itself.

Besides this favorable biogeochemical impact on the global climate system, afforestation affects also the regional climate by changing the biogeophysical characteristics of the land surface (Pielke et al., 2011; Bright et al., 2017). In general, the albedo of forests is lower than of other natural land covers. As a result, more shortwave radiation is absorbed, counteracting the increased OLR (Bala et al, 2007; Bonan, 2008). Thus, the regional climate effect of afforestation depends on the weighting between biogeochemical changes of the longwave radiation balance and biogeophysical changes of the shortwave radiation balance (Claussen et al., 2001; Pielke et al., 2011).

Moreover, biogeophysical changes with afforestation have also a direct effect on the longwave radiation balance. By changing land surface characteristics like albedo, surface roughness or leaf area index, surface temperatures are altered (Lee et al., 2011; Duveiller et al., 2018). Since longwave radiation emissions from the surface are, according to the Stefan-Boltzmann law, a function of the surface temperature (T_s), changes in the longwave radiation emissions follow (Vargas Zeppetello et al.,

2019). Moreover, changes in the land surface characteristics with afforestation generally lead to an increase of the turbulent heat fluxes (Burakowski et al., 2018; Breil et al., 2020). Atmospheric temperatures (T_a) are consequently increased (Alkama & Cescatti, 2016; Breil et al., 2020), which in turn affect the longwave radiation emitted by the atmosphere. Furthermore, changes in the evapotranspiration rates alter the water vapor concentrations in the atmosphere (Q_a) (Bonan, 2008). Since water vapor is known to be an important greenhouse gas, changes in its concentrations also affect the atmospheric longwave radiation emissions (Claussen et al., 2001; Swann et al., 2010).

In spite of their relevance, these complex biogeophysically induced changes in the longwave radiation balance are generally not considered in the ongoing debate on afforestation as a regional mitigation strategy. In general, studies mainly emphasize the effects of the biogeochemically induced CO_2 reduction and the biogeophysically induced changes in the albedo (Claussen et al., 2001; Bala et al, 2007). An all-inclusive understanding of the interrelation between afforestation and the longwave radiation balance is thus missing. The arising question whether biogeophysical changes are regionally strengthening or weakening the favorable biogeochemical impact of afforestation on the longwave radiation balance is thus not yet answered. The goal of this study is to disentangle the contribution of both biogeochemical and biogeophysical processes on the emitted longwave radiation over Europe, in a step towards a physically based comprehensive assessment of afforestation as a regional mitigation strategy to climate change.

The study is embedded in the Land Use and Climate Across Scales (LUCAS) project (Davin et al., 2020). LUCAS aims to investigate the impact of land use changes on the European climate by performing Regional Climate Model (RCM) simulations. In the first phase of the project, idealized afforestation experiments were performed. In one experiment, the whole European continent was covered by forest (FOREST), in the other experiment the whole continent was covered by grassland (GRASS). By means of these idealized simulations, the maximum possible effect of afforestation on the European climate could be estimated (Davin et al., 2020; Breil et al., 2020). However, only biogeophysical effects of afforestation are considered in these simulations, since the carbon cycle is generally not included in RCMs. Thus, the removal of CO_2 from the atmosphere was not taken into account.

In order to close this gap, an additional FOREST simulation which considers the reduced CO_2 concentrations with afforestation (CARBON) is analyzed. By comparing the results of CARBON, FOREST and GRASS with the results of an offline radiative transfer model, the respective contributions of biogeochemical and biogeophysical processes to the regional climate system, and particularly to the longwave radiation balance, can be quantified. Section 2 describes the used methodology. The main results are presented (section 3), followed by the discussion (section 4) and conclusions (section 5).

2. Methods

2.1. RCM simulations

All simulations (GRASS, FOREST, CARBON) are performed with the RCM CCLM-VEG3D (Breil et al., 2021) for the Coordinated Downscaling Experiment – European Domain (EURO-CORDEX; Jacob et al., 2014) on a horizontal resolution of 0.44° (~50 km). The simulations were driven by ERA-Interim reanalyses (Dee et al., 2011) at the lateral boundaries and the lower boundary over sea. The simulation period is 1986–2015. A spin-up of 7 years was performed before 1986. For this spin-up, CCLM-VEG3D was again driven with ERA-Interim reanalyses for the period 1979-1985, whereby the same model setup was used as for the period 1986-2015. The simulated conditions in the soil and in the atmosphere at the end of the spin-up period were then used as initial conditions in the long-term simulation.

The applied land use datasets are derived from a MODIS-based present-day land cover map (Lawrence and Chase, 2007), in which the land use classes in each grid cell were set to forest (FOREST, CARBON) or grassland (GRASS), respectively, excluding deserts and glaciers (Davin et al., 2020). In CARBON, the resulting reduction in global CO_2 concentrations by an idealized Europe-wide afforestation (see section 2.2) is implemented in CCLM-VEG3D, replacing the historic CO2 concentrations used in FOREST and GRASS.

2.2. Carbon sequestration by an idealized Europe-wide afforestation

In this idealized afforestation experiment, the whole European continent is afforested, starting from a continent entirely covered with grassland. Fig. 1 shows the respective partitioning of the afforested area in boreal and temperate forests. In this experiment, 405 million hectares of Europe are covered with boreal forests, 848 million hectares with temperate forests, thus 1.253 billion hectares in total. On the basis of recent forest inventory data and the results of long-term ecosystem studies, Pan et al. (2011) estimated the amount of carbon sequestrated (biomass + soil) in boreal forests to 239 MgC per hectare, and 155 MgC per hectare in temperate forests. This yields a total amount of 228.3 PgC sequestrated by a Europe-wide afforestation.

The arising global CO_2 concentrations from this idealized afforestation are calculated according to an analytical approach of Goodwin et al. (2007). Assuming a mature forest and steady-state conditions between the atmosphere and the buffering ocean-mixed-layer on a centennial timescale, changes in the atmospheric CO_2 partial pressure P_{CO2} are calculated as follows:

$$\Delta P_{CO_2} = \int_{\Sigma C_1}^{\Sigma C_2} \frac{P_{CO_2}}{I_B} d\Sigma C \qquad \text{Eq. (1),}$$

where I_B is the total carbon inventory of the atmosphere plus the total buffered carbon inventory of the ocean. $d\Sigma C$ is the change in the total amount of carbon in the atmosphere-ocean system. Assuming

furthermore that changes in I_B are small compared to the total buffered inventory, Eq. (1) can be integrated to

$$P_{CO_2} = P_i \, e^{\frac{\Delta\sum C}{I_B}} \quad \text{Eq. (2),}$$

where P_i is the initial partial pressure of carbon dioxide at pre-industrial conditions. $\Delta\Sigma C$ is the difference between the total anthropogenic carbon emissions until the year 1986 when our simulation starts (based on Gütschow et al., 2019), and the amount of carbon that would have been removed from the atmosphere by an idealized Europe-wide afforestation. Terrestrial emissions caused by land use changes are not considered, since land emissions are balanced by the terrestrial CO_2 sink of enhanced plant growth and the lengthening of the growing season (Friedlingstein et al., 2020).

According to Eq. (2), a resulting global CO_2 concentration of 279 ppm is calculated, constituting an equilibrium on a centennial timescale. Thus, an idealized Europe-wide afforestation, starting from a continent entirely covered with grassland, would have reduced the global CO_2 concentrations at the beginning of our simulation period from 347 ppm in 1986 to pre-industrial levels. This global CO_2 concentration is then implemented in the CARBON simulation. Differences in the CO_2 concentrations between a grassland continent and historic CO_2 concentrations are not considered, in order to enable a direct comparison of the CARBON simulation with the GRASS and FOREST runs, and thus, a consistent decomposition of biogeophysical and biogeochemical effects of afforestation. As a consequence, the CO2 induced global climate feedbacks are not taken into account.

2.3. BUGSrad

Longwave radiation (DLR and OLR) is an implicit function of T_s, T_a, Q_a and the CO_2 concentrations. While the individual contribution of CO_2 on changes in DLR and OLR can be derived from the difference between CARBON and FOREST, such an attribution is not possible for T_s, T_a and Q_a. Thus, DLR and OLR are additionally recalculated with the offline radiative transfer model BUGSrad (Stephens et al., 2001). BUGSrad solves the radiative transfer equation under the assumption of a plane-parallel atmosphere as proposed by Ritter and Geleyn (1992). Thus, BUGSrad is using the same radiative transfer scheme as it is implemented in CCLM-VEG3D, enabling a direct comparison with the RCM results. However, the radiative schemes in CCLM-VEG3D and BUGSrad are not completely identical. BUGSrad is set up with 6 shortwave and 12 longwave bands, whereas CCLM-VEG3D is set up with 3 shortwave and 5 longwave bands.

The calculations in BUGSrad are based on mean seasonal profiles of T, Q and pressure simulated in CCLM-VEG3D. Only clear-sky situations (daily mean cloud fraction < 20%) are considered, in order to exclude interfering influences of clouds on the longwave radiation balance. Emissions from the lowest atmospheric level correspond to DLR and emission from the uppermost level correspond to OLR. The

calculations are performed for eight different European sub-regions, adopted from the PRUDENCE project (Christensen & Christensen, 2007), shown as red rectangles in Fig. 1.

The advantage of such an offline model is that numerous simulations can be performed, in which each component affecting DLR and OLR, can be individually varied. In this way, the sensitivity of DLR and OLR to changes in T_s, T_a and Q_a can be quantified. Subsequently, the respective proportion of each component to changes in DLR and OLR can be quantified by means of a Taylor expansion, whereby the derived sensitivities from the offline simulations constitute the partial derivatives of the Taylor expansion (Shine & Sinha, 1991; Huang et al., 2007). Finally, the individual contributions of T_s, T_a and Q_a to the simulated afforestation effects on DLR and OLR with CCLM-VEG3D are derived by multiplying the changes in the temperature and humidity profiles with the partial derivatives of T_s, T_a and Q_a.

3. Results

3.1. CCLM-VEG3 results

3.1.1. Effects on mean annual surface temperatures

Fig. 2a shows the differences in DLR between CARBON and FOREST over the whole simulation period. Differences between both RCM simulations are only caused by the regional biogeochemical effects in Europe of afforestation. DLR is reduced in CARBON across Europe, as a result of the reduced CO_2 concentrations. This reduced DLR leads to slightly reduced yearly mean T_s in CARBON (Fig. 2b). However, the impact of this biogeochemical effect on T_s is negligible in comparison to the biogeophysically induced changes of T_s (Fig. 2c and Fig. 2d). Fig. 2c shows the differences between FOREST and GRASS for the yearly mean T_s in Europe. Differences between these simulations are only caused by biogeophysical changes with afforestation. The magnitude of the differences between FOREST and GRASS is much higher than between CARBON and FOREST, where only biogeochemical effects are considered. For instance, the biogeochemical effects of afforestation (CARBON-FOREST) lead to a reduction of the mean annual T_s of about -0.06 K in Scandinavia and -0.03 K at the Iberian Peninsula, while the biogeophysical effects (FOREST-GRASS) result in a mean warming of 1.06 K in Scandinavia and a mean cooling of -0.77 K at the Iberian Peninsula. The differences between CARBON and GRASS (Fig. 2d), which can be considered as the total effect of afforestation, since both biogeochemical and biogeophysical processes are taken into account, are consequently mainly caused by biogeophysical processes and of the same magnitude as the differences between FOREST and GRASS (1.0 K in Scandinavia and -0.8 K at the Iberian Peninsula). Thus, even with an idealized reduction of the global CO_2 concentrations to pre-industrial levels by a Europe-wide afforestation, the regional climate response to afforestation would be mainly dominated by biogeophysical effects.

3.1.2. Effects on the mean seasonal surface temperatures

The mean seasonal differences in T_s between the CARBON and the GRASS simulation are shown in Fig. 3. In the winter season (December to February; DJF), warmer T_s is simulated almost all over Europe except of the Iberian Peninsula (IP, Fig. 3a). In contrast to this warmer T_s in winter, T_s is reduced in summer (June to August; JJA) all over Europe with afforestation (Fig. 3b).

The warmer T_s in winter is caused by the masking effect of snow on trees (Essery, 2013). In the case of a snow cover, forests are only partially masked by snow due to their large vegetation height, while grasslands are completely covered with snow. As a result, forests absorb more solar radiation than grasslands in winter, and thus, more energy is available to heat up the vegetation surface. On the Iberian Peninsula, snow is generally not occurring in winter and the differences in absorbed solar radiation are consequently not that strong than for the rest of Europe. Since latent heat fluxes of forests are simultaneously increased in IP in winter (Fig. 4a), a larger part of the incoming radiative energy can be released into the atmosphere and surface temperatures are reduced.

In summer, forests are able to efficiently transform the radiative energy input at the surface into increased latent heat (Fig. 4b) and sensible heat fluxes, due to their higher surface roughness, higher biomass and deeper root system in comparison to grasslands. Thus, more turbulent energy is removed from the vegetation surface and transported into the atmosphere than for grasslands (Fig. 4c), with the consequence that all over Europe T_s is reduced in summer with afforestation (Fig. 3b; Burakowski et al., 2018; Breil et al., 2020).

3.1.3. Effects on the longwave radiation balance

Fig. 5 shows the differences between the CARBON and the GRASS simulation for DLR (a+c) and OLR (b+d) for the winter season (a+b) and the summer season (c+d). In winter, DLR is enhanced all over Europe by afforestation, except of IP. This extensive increase in DLR is counterintuitive, since one would rather expect a reduction in DLR due to the reduced atmospheric CO_2 concentrations with afforestation. OLR is also increased in winter all over Europe, which is in turn in line with the reduced atmospheric CO_2 concentrations. In summer, a dipole in the DLR differences between CARBON and GRASS is simulated, with a reduced DLR in central and southern Europe and an increased one in Scandinavia (SC). A similar spatial pattern is simulated for OLR in summer with slightly increased (reduced) OLR in northern Europe (southern Europe).

In order to be able to explain these spatial longwave radiation patterns, DLR and OLR are additionally simulated with the offline radiative transfer model BUGSrad. By means of a linearization of these BUGSrad simulations, the respective contributions of biogeophysical (changes in the surface temperatures, atmospheric temperatures and atmospheric water vapor concentrations) and biogeochemical (reduced CO2 concentrations) processes with afforestation on the longwave radiation balance can be decomposed.

3.2. BUGSrad results

3.2.1. Effects on the longwave radiation balance

Fig. 6 shows the differences in DLR (a+c) and OLR (b+d) for the winter (a+b) and the summer season (c+d) between CARBON and GRASS simulated with the BUGSrad radiative transfer model. The blue bars show the total differences in DLR or OLR calculated by the offline model. The other colored bars show the respective contributions of CO_2 (pink), Q_a (green), T_a (yellow) and T_s (black) to changes in DLR and OLR between CARBON and GRASS. Thus, the black, yellow and green bars represent the biophysical effects on the longwave radiation balance with afforestation, the pink bars the biogeochemical ones. The grey bar is the residuum, which is attributed to non-linear effects.

The simulated differences between CARBON and GRASS with BUGSrad are in good agreement with the results of CCLM-VEG3D (see Fig. 5). The calculated tendencies of afforestation are similar for the different regions and seasons. BUGSrad is also simulating a Europe-wide increase in DLR (except of IP) and OLR in winter in accordance with CCLM-VEG3D (see Fig. 6a, 6b and Fig. 5a, 5b). The radiative dipole in summer with increased DLR and OLR in northern Europe and reduced DLR and OLR in southern Europe is also consistently simulated with both models (see Fig. 6a, 6b and Fig. 5a, 5b). However, the absolute simulated differences between CARBON and GRASS can be different in some regions or seasons. For instance, the reduction in OLR in SC in summer with afforestation is stronger pronounced in BUGSrad (Fig. 6d) than in CCLM-VEG3D (Fig. 5d), which is also the case for the reduction in DLR in winter in IP (see Fig. 6a, 5a). These differences are most likely caused by the different numbers of shortwave and longwave bands in CCLM-VEG3D and BUGSrad.

The linearization of the differences in longwave radiation between CARBON and GRASS with BUGSrad reveals that the increased DLR with afforestation in winter is primarily a result of biogeophysical effects, compensating the attenuating effect of reduced CO_2 concentrations (negative pink bars) on DLR (Fig. 6a). In this context, especially T_s has a strong impact on the differences in DLR (positive black bars). Warmer T_s in winter (Fig. 3a) increase the longwave radiation emitted from the surface (except of IP where T_s is reduced). As a result, more longwave radiation can be absorbed by the atmosphere and reemitted as DLR to the surface. This positive feedback on the DLR is amplified by a generally warmer T_a, which is caused by the increased radiative energy input in winter. In addition, Q_a is increased in Europe, because of the higher evapotranspiration rates of forests in comparison to grasslands (Fig. 4a). Both, warmer T_a and higher Q_a have a reinforcing effect on DLR (positive yellow and green bars). Thus, DLR is enhanced in winter with afforestation although the CO_2 concentrations are reduced.

The same biogeochemical and biogeophysical changes of the longwave radiation balance lead to an increase in OLR (Fig. 6b). The increased longwave radiation emissions, caused by the increased T_s,

provide more radiative energy that can be released into space (positive black bars). Simultaneously, more longwave radiation can escape the atmosphere, due to reduced CO_2 concentrations (positive pink bars). Therefore, biophysical and biochemical processes amplify each other, resulting in increased OLR given afforestation all over Europe.

In contrast to the increased T_s in winter, T_s is reduced in summer with afforestation (Fig. 3b). The longwave radiation emitted from the surface is consequently reduced and less radiative energy can be absorbed and reemitted by the atmosphere (negative black bars in Fig. 6c). In combination with the reduced CO_2 concentrations (negative pink bars), DLR is therefore reduced all over Europe, except of SC (Fig. 6c). There, the T_s reduction with afforestation is quite small (Fig. 3b) and the reduction of longwave radiation emitted from the surface is not as clear as for other areas (slightly negative black bar), thus remaining on a comparatively high level. Additionally, evapotranspiration is strongly increased in SC in summer (Fig. 4b), leading to increased Q_a in the lower troposphere (not shown). Since water vapor is an effective greenhouse gas, increased concentrations contribute to an enhanced absorption of the (just slightly reduced) longwave radiation emitted by the surface (clearly positive green bar in SC). In this way, the biogeophysically induced changes of DLR compensate the attenuating effect of reduced CO_2 concentrations on DLR in SC (negative pink bar).

Fig. 6d shows that biogeophysical and biogeochemical changes with afforestation have opposing effects on OLR during summer. However, colder T_s reduce the longwave radiation emissions from the surface, and thus the radiative energy that can be released into space (negative black bars). On the other hand, reduced CO_2 concentrations in the atmosphere lead to a reduced absorption of longwave radiation and more radiation that can pass the atmosphere (positive pink bars). Over central Europe (ME), both processes balance each other leading to a net zero effect. In northern Europe (SC, BI), biogeochemical effects are dominating, since changes in T_s and thus, the longwave radiation emissions are especially in SC quite small. This process is stronger pronounced in BUGSrad than in CCLM-VEG3D. Over southern and eastern Europe (MD, EA), the impact of the biogeophysical changes on OLR is dominating. Here, the reduced longwave radiation emissions of the colder surface are amplified by increased Q_a in the mid-troposphere (not shown), counteracting the effect of the reduced CO_2 concentrations.

3.3. TOA Energy Balance

The decomposition of the BUGSrad simulations showed that biogeophysical effects of afforestation have a strong impact on the longwave radiation balance, which does consequently not only depend on the removal of CO_2 from the atmosphere. In considering both biogeophysical and biogeochemical effects, the question arises, whether afforestation has in general a warming or a cooling effect on the regional climate in Europe. Since the regional climate conditions in Europe depend decisively both on

the lateral heat transport and on the radiative energy input, the energy balance at the top of the atmosphere (TOA) is analyzed to quantify the impact of the latter. With this aim, the net longwave radiation leaving the earth system is subtracted from the net shortwave radiation input into the system. In this way, biogeophysical changes in the shortwave radiation balance with afforestation by a reduced surface albedo can be related to changes in the longwave radiation balance, which is affected by both biogeophysical and biogeochemical process, as demonstrated above.

Changes in the TOA energy balance between CARBON and GRASS are shown for (a) winter, (b) summer and (c) the whole year in Fig. 7. Red areas indicate regions in which afforestation leads to an increased energy input into the regional climate system in Europe, blue areas indicate regions with a reduced energy input. In winter, the TOA energy balance is increased in southern Europe, the Alpine region, eastern Europe and southern Scandinavia (Fig. 7a). In these regions, the increased longwave radiative energy loss by an increased OLR is compensated by an increased shortwave radiation input. In central Europe, the British Isles and northern Scandinavia, the opposite is the case and the TOA energy balance is decreased or close to zero.

In summer, the interplay between changes in OLR and changes in the shortwave radiation lead to a decreased TOA energy balance in central and north-eastern Europe and a strongly increased energy balance in southern Europe as well as parts of Scandinavia (Fig. 7b). Across seasons, the TOA energy balance is almost all over Europe increased with afforestation (Fig. 7c). The increased TOA energy balance in Scandinavia is explained by a strong increase in the net shortwave radiation in spring (Fig. 8), due to differences in the snow cover. Afforestation is consequently associated with an increased TOA energy balance over Europe.

4. Discussion

Prior to the CARBON simulation, a global atmospheric CO_2 concentration of 279 ppm was calculated as a response to a Europe-wide afforestation at the beginning of our simulation period (1986, see section 2.2). At first glance, this substantial reduction of the global CO_2 concentration to pre-industrial levels is astonishing. However, it has to be considered that the applied method is designed for a mature forest, under the assumption of an equilibrium in the atmosphere-ocean system, which will be achieved only on centennial timescales (Goodwin et al., 2007). An inertial short-term adjustment of the CO_2 concentrations is therefore not considered. In addition, the presented study is an idealized and simplified afforestation experiment, starting from a grassland continent. Thus, it is not a realistic afforestation scenario (Bastin et al., 2019) and areas are afforested, in which the environmental conditions are not actually ideal. Changes in the environmental conditions due to climate change are also not considered. Moreover, ongoing fossil fuel emissions are neglected (Jones et al., 2016) and the carbon already stored in grasslands (soil + biomass) is also not taken into account (Jackson et al., 2002).

The real carbon sequestration potential of afforestation should consequently be lower and the reduction in global CO_2 concentrations, associated with a more realistic afforestation scenario, should thus be smaller. Hence, this also means that the effect of biogeophysical processes on the longwave radiation balance is likely to be even stronger in comparison to biogeochemical processes. Thus, the regional warming effect of afforestation in Europe is expected to be even more intense in a realistic setup. This experiment should thus be considered as sensitivity study by which the maximum potential effect of afforestation on the longwave radiation balance and the regional climate was estimated.

Such a quantification of the direct impacts of biogeophysical and biogeochemical processes on changes in the longwave radiation balance with afforestation is only possible within idealized RCM simulations, since the indirect effects of global climate feedbacks can be specifically excluded. Moreover, the advantage of RCM simulations is that the physical processes related to the interactions between the land surface (soil and vegetation) and the atmosphere are better resolved than in global climate simulations, whereby relevant land-atmosphere feedbacks are simulated more accurately on the regional scale.

However, not all effects of afforestation on the European climate can be fully described on the basis of the applied RCM approach. First, CO_2 dynamics are not considered in the CCLM-VEG3D simulations, since no carbon cycle (Liski et al., 2005) is implemented in the modeling framework. Furthermore, all simulations are driven by ERA-Interim reanalysis, which means present-day atmospheric conditions with recent CO_2 concentrations. The feedbacks of reduced CO_2 concentrations and biogeophysical effects on the global climate system, especially on ocean-atmosphere interactions (Davin & de Noblet-Ducoudré 2010; Swann et al., 2012) as well as on snow and sea ice cover (Donohoe et al., 2014), are consequently not considered.

These missing global feedbacks are most likely the reason for the small effects on simulated T_s in Europe by an atmospheric CO_2 reduction to pre-industrial levels (Fig. 2b). This small temperature effect is apparently in contradiction to observations, documenting that increasing CO_2 concentrations led to a considerable warming of up to 1.5 K in Europe until the end of our simulation period in comparison to pre-industrial levels (EEA, 2017). However, the results of our simulations are in line with recent studies providing evidence that the temperature effect of changing CO_2 concentrations is not mainly caused by direct changes in the longwave radiation balance, but by changes in the shortwave radiation balance, which are indirectly induced by changes in global CO_2 climate feedbacks, e.g. ice-albedo feedback associated with changes in the snow and ice cover (e.g., Donohoe et al., 2014). Since such feedbacks are not included in our experiment, we have to conclude that the driving boundary conditions of our simulations are too warm.

Based on the above, we can assume that an idealized reduction of the global CO_2 concentrations to pre-industrial conditions by a regional afforestation would have a global cooling effect, due to the

global climate feedbacks described above. A consideration of such colder global climate conditions in our experiment would of course have certain implications on the biogeophysical processes in our modeling domain. For instance, driving the CARBON simulation with generally colder boundary conditions would enhance snowfall during winter in Europe. The snow masking effect would consequently be increased and more solar radiation would be absorbed than with present-day boundary conditions. As a result, the TOA energy balance would be further enhanced in winter. This process is already known to be the reason for the general warming effect of afforestation in the high latitudes (e.g. Claussen et al., 2001; Bonan, 2008). Furthermore, more snow accumulation in winter would extend the melting phase in spring and increase the differences in absorbed solar radiation between CARBON and GRASS. Since an increased net shortwave radiation in spring (Fig. 8) is already an important factor for the increased TOA energy balance with afforestation particularly in Scandinavia, the total warming would be intensified.

In addition, the impact of wind sheer on the turbulent heat exchange is getting stronger for colder atmospheric conditions, since buoyance becomes smaller (e.g. Breil et al., 2021). That means that the impact of the surface roughness on T_s also becomes stronger. Since the surface roughness of forests is higher than of grasslands, the summertime cooling effect of afforestation on T_s (Fig. 3b) would be increased and emitted longwave radiation would be further reduced. Therefore, the consideration of global climate feedbacks in our modeling approach and thus, a forcing with colder boundary conditions, would even intensify the increased TOA energy balance and the warming effect of afforestation in Europe. An idealized reduction of the global CO_2 concentrations to pre-industrial levels by afforestation would consequently not actually cool the regional climate in Europe to pre-industrial conditions, as the regionally increased TOA energy balance would counteract the global effect.

However, all derived results are model dependent and are therefore associated with uncertainties. For instance, the study of Davin et al., (2020) showed that the response of different RCMs to afforestation can be quite different for some climatological quantities like evapotranspiration. For Ts, conversely, afforestation effects are very consistent across the models in Europe. In winter, afforestation generally leads to warmer temperatures, due to the snow masking effect of trees (Davin et al., 2020). In summer, increased turbulent heat fluxes into the atmosphere are consistently simulated with afforestation, generally resulting in a reduction of Ts in the models (Breil et al., 2020). Thus, the presented temperature responses are in good agreement with other modeling results. This is also the case for the simulated net shortwave radiation all over the year in Europe (Davin et al., 2020). Since Ts is according to the BUGSrad analysis the most relevant biogeophysical quantity for the net longwave radiation and thus, in combination with the net shortwave radiation, also for the TOA energy balance, this gives us confidence that our model results are robust.

5. Conclusions

In this study, the general effects of biogeophysical and biogeochemical processes on the longwave radiation balance and the regional climate conditions in Europe are analyzed within an idealized Europe-wide afforestation RCM experiment, in which the global CO_2 concentrations were reduced to pre-industrial levels at the beginning of our simulation period. The respective contributions of biogeophysical and biogeochemical effects were decomposed by means of additional offline simulations with a radiative transfer model.

Results show that the impact of biogeochemical processes with afforestation on surface temperature (T_s) is negligible in comparison to the biogeophysical effects (Fig. 2). Beyond that, biogeophysical processes affect the regional longwave radiation balance, which is generally thought to be positively influenced by afforestation, due to the net removal of CO_2 from the atmosphere. However, our results provide evidence that biogeophysically induced changes of T_s, T_a and Q_a are at least as important for the longwave radiation balance as the atmospheric CO_2 reduction (Fig. 5 and 6). In particular, the changes in T_s have a considerable impact on the magnitude of the longwave radiation, in line with Vargas Zeppetello et al. (2019).

While results based on coarser resolved global climate studies rather indicate so far that biogeophysical and biogeochemical effects balance each other in Europe (Claussen et al., 2001, Bala et al., 2007), we provide here evidence that afforestation as implemented in our simulations has a total warming effect on the regional climate (Fig. 7). Thus, the increased shortwave radiation input due to the biogeophysical reduction of the surface albedo, is not compensated by increased longwave radiation emissions, associated with reduced CO_2 concentrations. Even with an idealized reduction of the global CO_2 concentrations to pre-industrial levels, the European climate response would still be dominated by biogeophysical processes associated with Europe-wide afforestation. A sole consideration of forests carbon sequestration potential is therefore not enough to assess the suitability of afforestation as mitigation strategy. We conclude that biogeophysical effects always need to be taken into account comprehensively, particularly as they affect the outgoing longwave radiation, which is the reason for the generally positive assessment of afforestation as mitigation strategy.

Code availability

The code of CCLM-VEG3D is available upon request from the corresponding author. The code of BUGSrad is available on the BUGSrad GitHub repository (https://github.com/mattchri/BUGSrad, last access: 16 November 2022).

Data availability

The data that support the findings of this study are available upon reasonable request from the corresponding author.

Author contribution

MB designed the study and wrote the paper. MB and FK performed the CCLM-VEG3D simulations and FK performed the BUGSrad simulations. FK analyzed the data and prepared the figures. All authors contributed with discussion, interpretation of results and text revisions.

Competing interests

The authors declare that they have no conflict of interest.

Financial Support

JGP thanks the AXA Research Fund for support.

Acknowledgements

All authors thank Peter Knippertz for the fruitful discussions and his scientific input.

References

Alkama, R., and Cescatti, A.: Biophysical climate impacts of recent changes in global forest cover. *Science*, *351*(6273), 600-604. DOI: 10.1126/science.aac8083, 2016.

Bala, G., Caldeira, K., Wickett, M., Phillips, T. J., Lobell, D. B., Delire, C., and Mirin, A.: Combined climate and carbon-cycle effects of large-scale deforestation. *Proceedings of the National Academy of Sciences*, *104*(16), 6550-6555. https://doi.org/10.1073/pnas.0608998104, 2007.

Bastin, J. F., Finegold, Y., Garcia, C., Mollicone, D., Rezende, M., Routh, D., Zohner, C., and Crowther, T. W.: The global tree restoration potential. *Science*, *365*(6448), 76-79. DOI: 10.1126/science.aax0848, 2019.

Bonan, G. B.: Forests and climate change: forcings, feedbacks, and the climate benefits of forests. S*cience*, *320*(5882), 1444-1449. DOI: 10.1126/science.1155121, 2008.

Burakowski, E., Tawfik, A., Ouimette, A., Lepine, L., Novick, K., Ollinger, S., Zarzycki, C., and Bonan, G.: The role of surface roughness, albedo, and Bowen ratio on ecosystem energy balance in the Eastern United States. *Agricultural and Forest Meteorology*, *249*, 367-376. https://doi.org/10.1016/j.agrformet.2017.11.030, 2018.

Breil, M., Davin, E. L., and Rechid, D.: What determines the sign of the evapotranspiration response to afforestation in European summer? *Biogeosciences*, *18*(4), 1499-1510. https://doi.org/10.5194/bg-18-1499-2021, 2021.

Breil, M., Rechid, D., Davin, E. L., de Noblet-Ducoudré, N., Katragkou, E., Cardoso, R. M., Hoffmann, P., Jach, L.L., Soares, P.M.M., Sofiadis, G., Strada, S., Strandberg, G., Tölle, M.H., and Warrach-Sagi, K.: The opposing effects of reforestation and afforestation on the diurnal temperature cycle at the surface and in the lowest atmospheric model level in the European summer. *Journal of Climate*, *33*(21), 9159-9179. https://doi.org/10.1175/JCLI-D-19-0624.1, 2020.

Bright, R. M., Davin, E., O'Halloran, T., Pongratz, J., Zhao, K., and Cescatti, A.: Local temperature response to land cover and management change driven by non-radiative processes. *Nature Climate Change*, *7*(4), 296-302. https://doi.org/10.1038/nclimate3250, 2017.

Christensen, J. H., and Christensen, O. B.: A summary of the PRUDENCE model projections of changes in European climate by the end of this century. *Climatic change*, *81*(1), 7-30. https://doi.org/10.1007/s10584-006-9210-7, 2007.

Claussen, M., Brovkin, V., and Ganopolski, A.: Biogeophysical versus biogeochemical feedbacks of large-scale land cover change. *Geophysical research letters*, *28*(6), 1011-1014. https://doi.org/10.1029/2000GL012471, 2001.

Davin, E. L., and de Noblet-Ducoudré, N.: Climatic impact of global-scale deforestation: Radiative versus nonradiative processes. *Journal of Climate*, *23*(1), 97-112. https://doi.org/10.1175/2009JCLI3102.1, 2010.

Davin, E. L., Rechid, D., Breil, M., Cardoso, R. M., Coppola, E., Hoffmann, P., Jach, L. L., Katragkou, E., de Noblet-Ducoudré, N., Radtke, K., Raffa, M., Soares, P. M. M., Sofiadis, G., Strada, S., Strandberg, G., Tölle, M. H., Warrach-Sagi, K., and Wulfmeyer, V.: Biogeophysical impacts of forestation in Europe: first results from the LUCAS (Land Use and Climate Across Scales) regional climate model intercomparison. *Earth System Dynamics*, *11*(1), 183-200. https://doi.org/10.5194/esd-11-183-2020, 2020.

Dee, D. P., Uppala, S. M., Simmons, A. J., Berrisford, P., Poli, P., Kobayashi, S., Andrae, U., Balmaseda, M. A., Balsamo, G., Bauer, P., Bechthold, P., Beljaars, A. C. M., van de Berg, L., Bidlot, J., Bormann, N., Delsol, C., Dragani, R., Fuentes, M., Geer, A. J., Haimberger, L., Healy, S. B., Hersbach, H., Holm, E. V., Isaksen, L., Kallberg, P., Köhler, M., Matricardi, M., McNally, A. P., Monge-Sanz, B. M., Morcrette, J.-J., Park, B.-K., Peubey, C., de Rosnay, P., Tavolato, C., Thepaut, J.-N., and Vitart, F.: The ERA-Interim reanalysis: Configuration and performance of the data assimilation system. *Quarterly Journal of the royal meteorological society*, *137*(656), 553-597. https://doi.org/10.1002/qj.828, 2011.

Donohoe, A., Armour, K. C., Pendergrass, A. G., and Battisti, D. S.: Shortwave and longwave radiative contributions to global warming under increasing CO2. *Proceedings of the National Academy of Sciences*, 111(47), 16700-16705, 2014.

Duveiller, G., Hooker, J., and Cescatti, A.: The mark of vegetation change on Earth's surface energy balance. *Nature communications*, *9*(1), 1-12. https://doi.org/10.1038/s41467-017-02810-8, 2018.

EEA, C. C.: Impacts and vulnerability in europe 2016–an indicator-based report. Luxembourg: Publications Office of the European Union, 1, 2017.

Essery, R.: Large-scale simulations of snow albedo masking by forests. *Geophysical Research Letters*, *40*(20), 5521-5525. https://doi.org/10.1002/grl.51008, 2013.

Friedlingstein, P., O'Sullivan, M., Jones, M. W., Andrew, R. M., Hauck, J., Olsen, A., Peters, G. P., Peters, W., Pongratz, J., Sitch, S., Le Quéré, C., Canadell, J. G., Ciais, P., Jackson, R. B., Alin, S., Aragão, L. E. O. C., Arneth, A., Arora, V., Bates, N. R., Becker, M., Benoit-Cattin, A., Bittig, H. C., Bopp, L., Bultan, S., Chandra, N., Chevallier, F., Chini, L. P., Evans, W., Florentie, L., Forster, P. M., Gasser, T., Gehlen, M., Gilfillan, D., Gkritzalis, T., Gregor, L., Gruber, N., Harris, I., Hartung, K., Haverd, V., Houghton, R. A., Ilyina, T., Jain, A. K., Joetzjer, E., Kadono, K., Kato, E., Kitidis, V., Korsbakken, J. I., Landschützer, P., Lefèvre, N., Lenton, A., Lienert, S., Liu, Z., Lombardozzi, D., Marland, G., Metzl, N., Munro, D. R., Nabel, J. E. M. S., Nakaoka, S.-I., Niwa, Y., O'Brien, K., Ono, T., Palmer, P. I., Pierrot, D., Poulter, B., Resplandy, L., Robertson, E., Rödenbeck, C., Schwinger, J., Séférian, R., Skjelvan, I., Smith, A. J. P., Sutton, A. J., Tanhua, T., Tans, P. P., Tian, H., Tilbrook, B., van der Werf, G., Vuichard, N., Walker, A. P., Wanninkhof, R., Watson, A. J., Willis, D., Wiltshire, A. J., Yuan, W., Yue, X., and Zaehle, S.: Global Carbon Budget 2020, *Earth Syst. Sci. Data*, 12, 3269–3340, https://doi.org/10.5194/essd-12-3269-2020, 2020.

Goodwin, P., Williams, R. G., Follows, M. J., and Dutkiewicz, S.: Ocean-atmosphere partitioning of anthropogenic carbon dioxide on centennial timescales. *Global Biogeochemical Cycles*, *21*(1), GB1014, https://doi.org/10.1029/2006GB002810, 2007.

Gütschow, J., Jeffery, L., Gieseke, R., and Günther, A.: The PRIMAP-hist national historical emissions time series (1850-2017). V. 2.1. GFZ Data Services. https://doi.org/10.5880/PIK.2019.018, 2019.

Harper, A. B., Powell, T., Cox, P. M., House, J., Huntingford, C., Lenton, T. M., Sitch, S., Burke, E., Chadburn, S. E., Collins, W. J., Comyn-Platt, E., Daioglou, V., Doelman, J. C., Hayman, G., Robertson, E., van Vuuren, D., Wiltshire, A., Webber, C. P., Bastos, A., Boysen, L., Ciais, P., Devaraju, N., Jain, A. K., Krause, A., Poulter, B., and Shu, S.: Land-use emissions play a critical role in land-based mitigation for Paris climate targets. *Nature communications*, *9*(1), 1-13. https://doi.org/10.1038/s41467-018-05340-z, 2018.

Huang, Y., Ramaswamy, V., and Soden, B.: An investigation of the sensitivity of the clear-sky outgoing longwave radiation to atmospheric temperature and water vapor. *Journal of Geophysical Research: Atmospheres*, *112*, D05104. https://doi.org/10.1029/2005JD006906, 2007.

592 Jackson, R. B., Banner, J. L., Jobbágy, E. G., Pockman, W. T., and Wall, D. H.: Ecosystem carbon loss with
593 woody plant invasion of grasslands. *Nature*, *418*(6898), 623-626.
594 https://doi.org/10.1038/nature00910, 2002.
595
596 Jacob, D., Petersen, J., Eggert, B., Alias, A., Christensen, O. B., Bouwer, L. M., Braun, A., Colette, A.,
597 Deque, M., Georgievski, G., Georgopoulou, E., Gobiet, A., Menut, L., Nikulin, G., Haensler, A.,
598 Hempelmann, N., Jones, C., Keuler, K., Kovats, S., Kröner, N., Kotlarski, S., Kriegsmann, A., Martin, E.,
599 van Meijgaard, E., Moseley, C., Pfeifer, S., Preuschmann, S., Radermacher, C., Radtke, K., Rechid, D.,
600 Rounsevell, M., Samuelsson, P., Somot, S., Soussana J.-F., Teichmann, C., Valentini, R., Vautard, R.,
601 Weber, B., and Yiou, P.: EURO-CORDEX: new high-resolution climate change projections for European
602 impact research. *Regional environmental change*, *14*(2), 563-578. https://doi.org/10.1007/s10113-
603 013-0499-2, 2014.
604
605 Jones, C. D., Ciais, P., Davis, S. J., Friedlingstein, P., Gasser, T., Peters, G. P., Rogelj, J., van Vuuren, D. P.,
606 Canadell, J. G., Cowie, A., Jackson, R. B., Jonas, M., Kriegler, E., Littleton, E., Lowe, J. A., Milne, J.,
607 Shrestha, G., Smith, P., Torvanger, A., and Wiltshire, A.: Simulating the Earth system response to
608 negative emissions. *Environmental Research Letters*, *11*(9), 095012. doi:10.1088/1748-
609 9326/11/9/095012, 2016.
610
611 Lawrence, P. J., and Chase, T. N.: Representing a new MODIS consistent land surface in the Community
612 Land Model (CLM 3.0). *Journal of Geophysical Research: Biogeosciences*, *112*, G01023.
613 https://doi.org/10.1029/2006JG000168, 2007.
614
615 Lee, X., Goulden, M. L., Hollinger, D. Y., Barr, A., Black, T. A., Bohrer, G., Bracho, R., Drake, B., Goldstein,
616 A., Gu, L., Katul, G., Kolb, T., Law, B. E., Margolis, H., Meyers, T., Monson, R., Munger, W., Oren, R., Tha
617 Paw U, K., Richardson, A. D., Schmid, H.-P., Staebler, R., Wofsy, S., and Zhao, L.: Observed increase in
618 local cooling effect of deforestation at higher latitudes. *Nature*, *479*(7373), 384-387.
619 https://doi.org/10.1038/nature10588, 2011.
620
621 Liski, J., Palosuo, T., Peltoniemi, M., and Sievänen, R.: Carbon and decomposition model Yasso for
622 forest soils. *Ecological modelling*, *189*(1-2), 168-182.
623 https://doi.org/10.1016/j.ecolmodel.2005.03.005, 2005.
624
625 Luyssaert, S., Ciais, P., Piao, S. L., Schulze, E. D., Jung, M., Zaehle, S., Schelhaas, M. J., Reichstein, M.,
626 Churkina, G., Papale, D., Abril, G., Beer, C., Grace, J., Loustau, D., Matteucci, G., Magnani, F., Nabuurs,

G. J., Verbeeck, H., Sulkava, M., van der Werf, G. R., Janssens, I. A., and members of the CARBOEUROPE-IP SYNTHESIS TEAM: The European carbon balance. Part 3: forests. *Global Change Biology*, *16*(5), 1429-1450. https://doi.org/10.1111/j.1365-2486.2009.02056.x, 2010.

Pan, Y., Birdsey, R. A., Fang, J., Houghton, R., Kauppi, P. E., Kurz, W. A., .Phillips, O. L., Shvidenko, A., Lewis, S. L., Canadell, J. G., Ciais, P., Jackson, R. B., Pacala, S. W., McGuire, A. D., Paio, S., Rautiainen, A., Sitch, S., and Hayes, D.: A large and persistent carbon sink in the world's forests. *Science*, *333*(6045), 988-993. DOI: 10.1126/science.1201609, 2011.

Pielke Sr, R. A., Pitman, A., Niyogi, D., Mahmood, R., McAlpine, C., Hossain, F., Goldewijk, K. K., Nair, U., Betts, R., Fall, S., Reichstein, M., Kabat, P., and de Noblet, N.: Land use/land cover changes and climate: modeling analysis and observational evidence. *Wiley Interdisciplinary Reviews: Climate Change*, *2*(6), 828-850. doi: 10.1002/wcc.144, 2011.

Ritter, B., and Geleyn, J. F.: A comprehensive radiation scheme for numerical weather prediction models with potential applications in climate simulations. *Monthly weather review*, *120*(2), 303-325. https://doi.org/10.1175/1520-0493(1992)120<0303:ACRSFN>2.0.CO;2, 1992.

Roe, S., Streck, C., Obersteiner, M., Frank, S., Griscom, B., Drouet, L., Fricko, O., Gusti, M., Harris, N., Hasegawa, T., Hausfather, Z., Havlik, P., House, J., Nabuurs, G.-J., Popp, A., Sanz Sanchez, M. J., Sanderman, J., Smit, P., Stehfest, E., and Lawrence, D.: Contribution of the land sector to a 1.5 C world. *Nature Climate Change*, *9*(11), 817-828. https://doi.org/10.1038/s41558-019-0591-9, 2019.

Shine, K. P., and Sinha, A.: Sensitivity of the Earth's climate to height-dependent changes in the water vapour mixing ratio. *Nature*, *354*(6352), 382-384. https://doi.org/10.1038/354382a0, 1991.

Stephens, G. L., Gabriel, P. M., and Partain, P. T.: Parameterization of atmospheric radiative transfer. Part I: Validity of simple models. *Journal of the atmospheric sciences*, *58*(22), 3391-3409. https://doi.org/10.1175/1520-0469(2001)058<3391:POARTP>2.0.CO;2, 2001.

Swann, A. L., Fung, I. Y., Levis, S., Bonan, G. B., and Doney, S. C.: Changes in Arctic vegetation amplify high-latitude warming through the greenhouse effect. *Proceedings of the National Academy of Sciences*, *107*(4), 1295-1300. https://doi.org/10.1073/pnas.0913846107, 2010.

Swann, A. L., Fung, I. Y., and Chiang, J. C.: Mid-latitude afforestation shifts general circulation and tropical precipitation. *Proceedings of the National Academy of Sciences*, *109*(3), 712-716. https://doi.org/10.1073/pnas.1116706108, 2012.

Vargas Zeppetello, L. R., Donohoe, A., and Battisti, D. S.: Does surface temperature respond to or determine downwelling longwave radiation? *Geophysical Research Letters*, *46*(5), 2781-2789. https://doi.org/10.1029/2019GL082220, 2019.

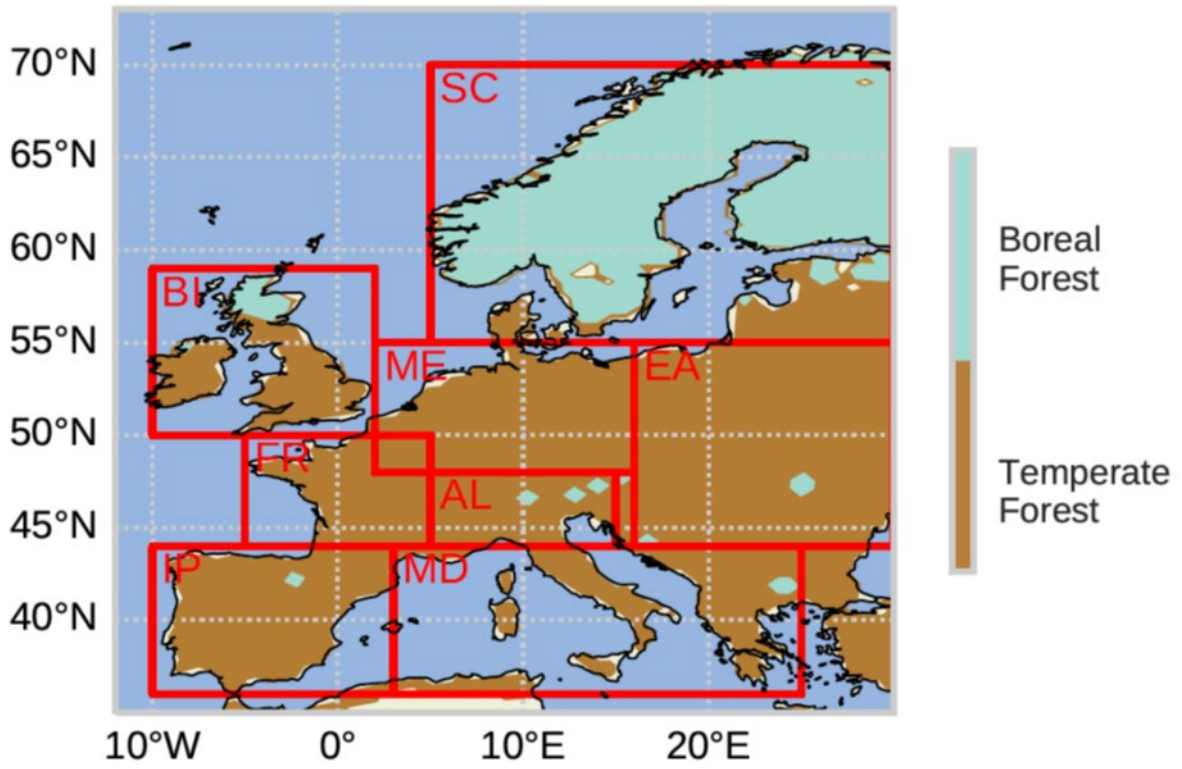

694

695 Figure 1: Spatial distribution of boreal and temperate forests in the CCLM-VEG3D FOREST and CARBON
696 simulations.

697

698

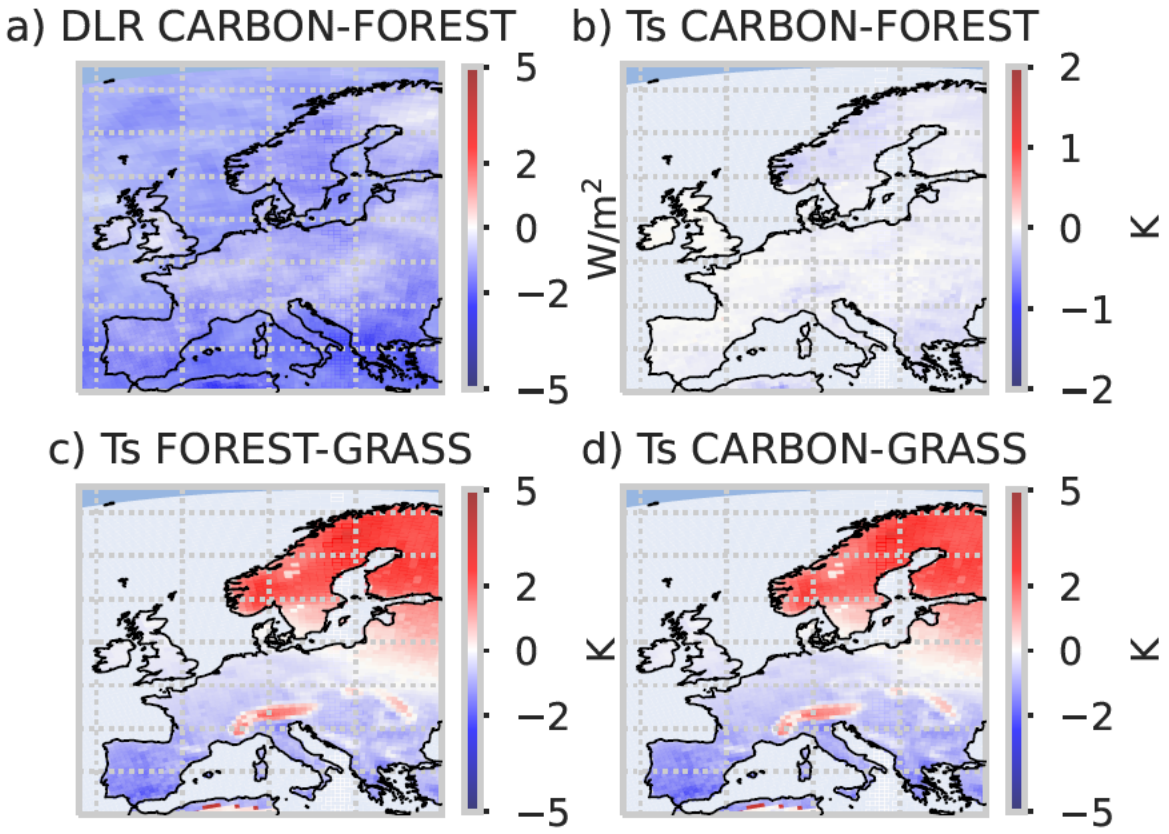

Figure 2: Yearly mean differences in (a) DLR between CARBON and FOREST, (b) T_s between CARBON and FOREST, (c) T_s between FOREST and GRASS, and (d) T_s between CARBON and GRASS for the period 1986-2015.

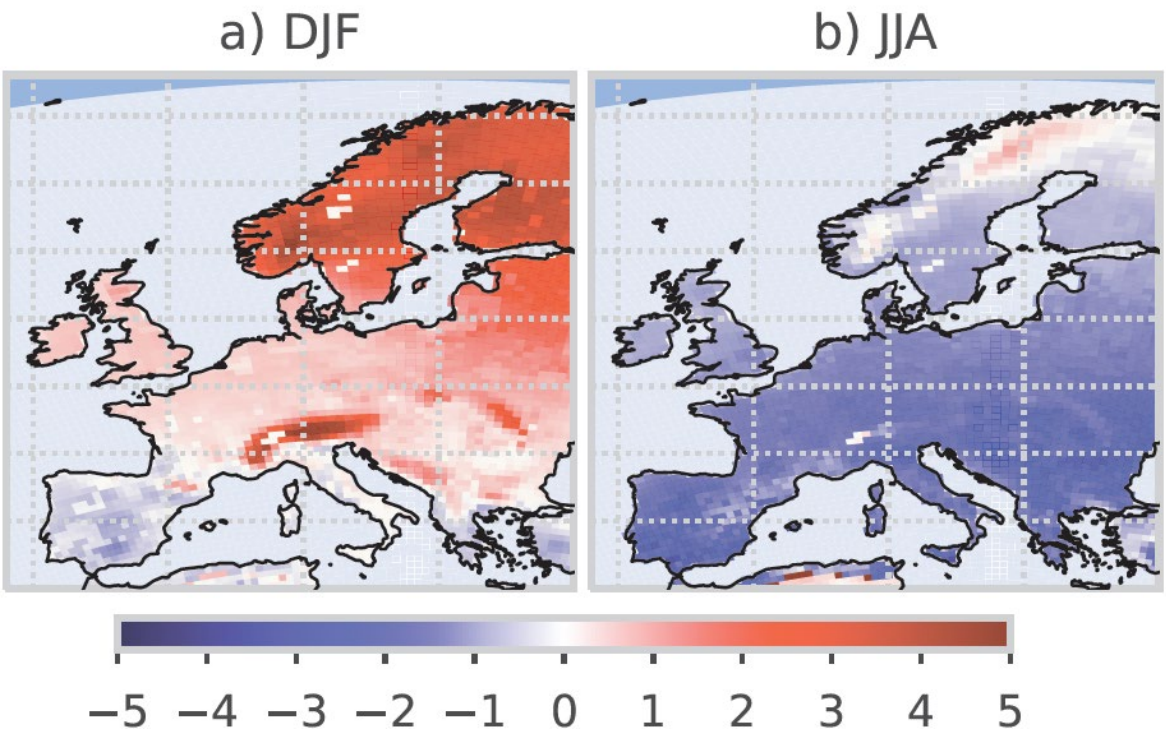

Figure 3: Mean differences in T_s in [K] between CARBON and GRASS for the period 1986-2015, for the (a) winter season and the (b) summer season.

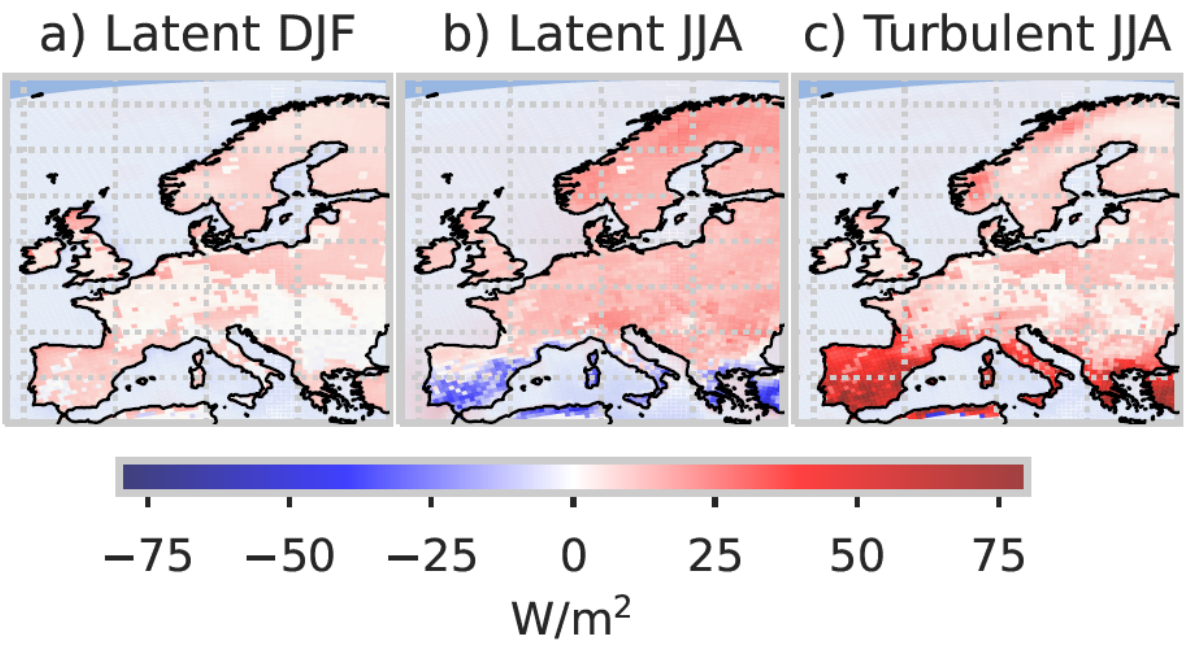

Figure 4: Mean differences between CARBON and GRASS for the latent heat fluxes in (a) winter and (b) summer for the period 1986-2015. The differences in the sum of all turbulent heat fluxes (latent + sensible) in summer is shown in (c).

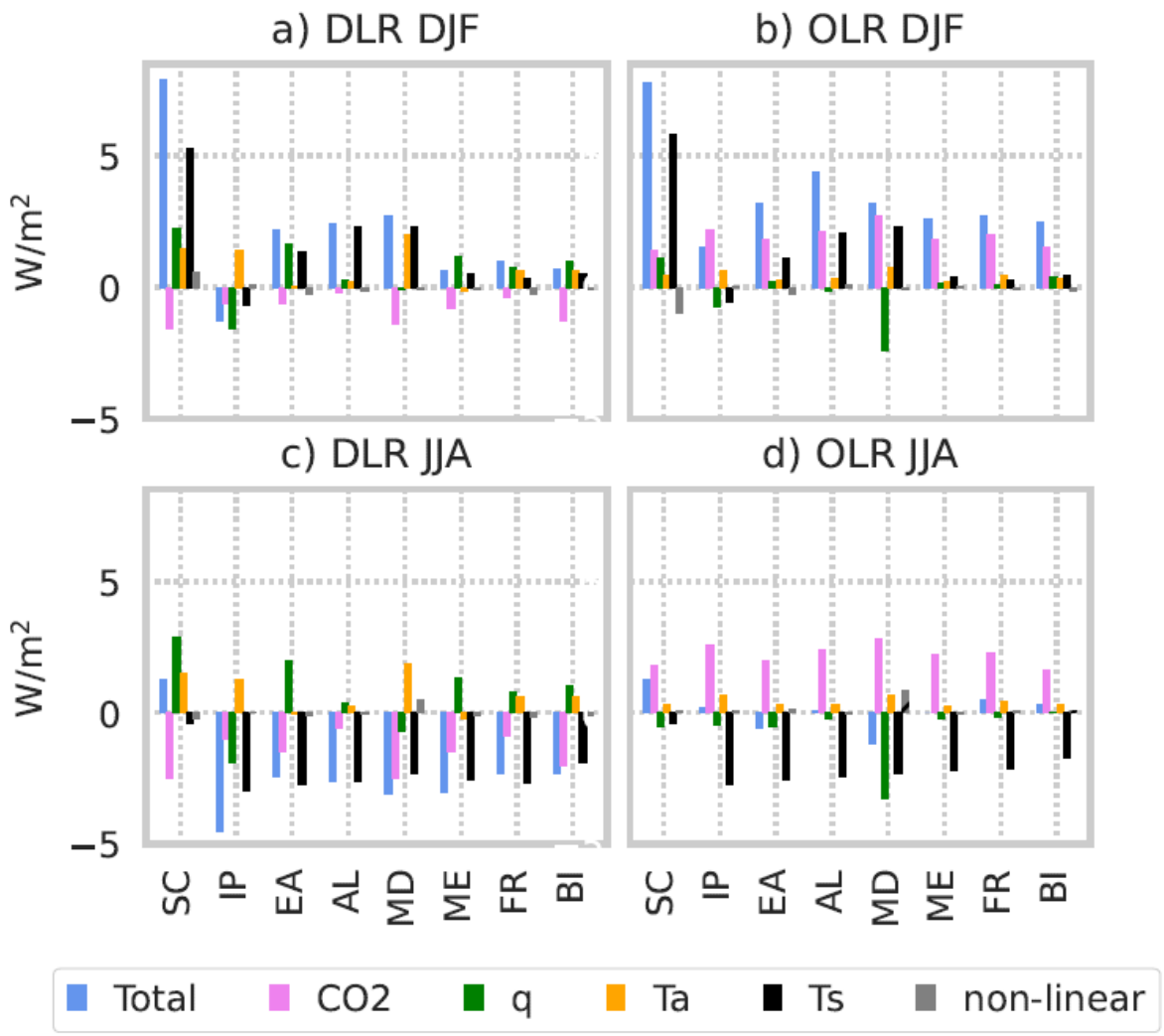

Figure 5: Differences in DLR (a+c) and OLR (b+d) for the winter (a+b) and the summer season (c+d) between CARBON and GRASS simulated with BUGSrad. Blue bars show total differences in DLR/OLR. The other bars show the respective contributions of CO_2 (pink), Q_a (green), T_a (yellow) and T_s (black) to changes in DLR/OLR. Black, yellow and green bars represent biogeophysical effects on the longwave radiation balance with afforestation, pink bars biogeochemical effects. The grey bar is the residuum, which is attributed to non-linear effects.

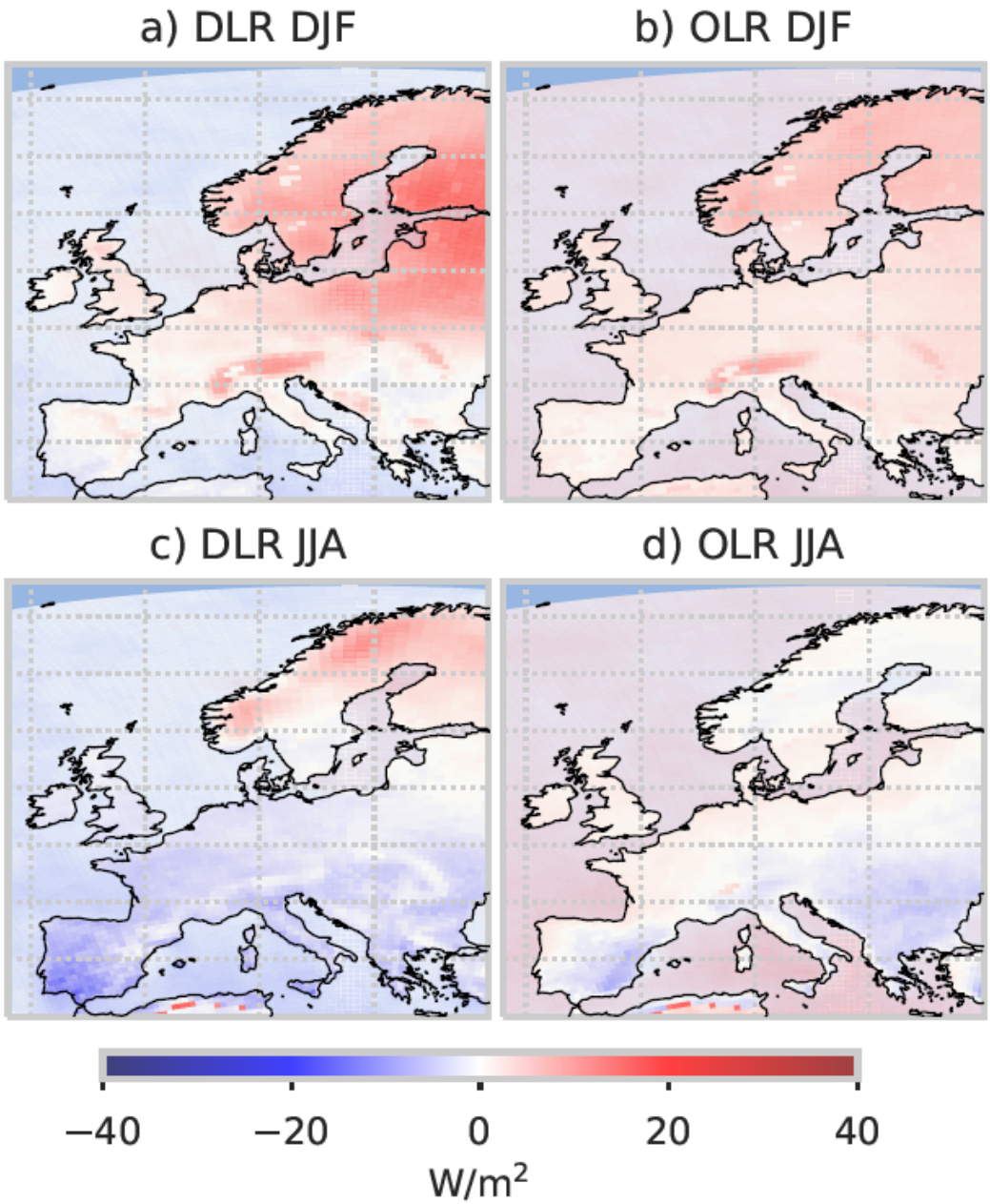

Figure 6: Differences between CARBON and GRASS for DLR (a+c) and OLR (b+d) for the winter season (a+b) and the summer season (c+d) over the period 1986-2015.

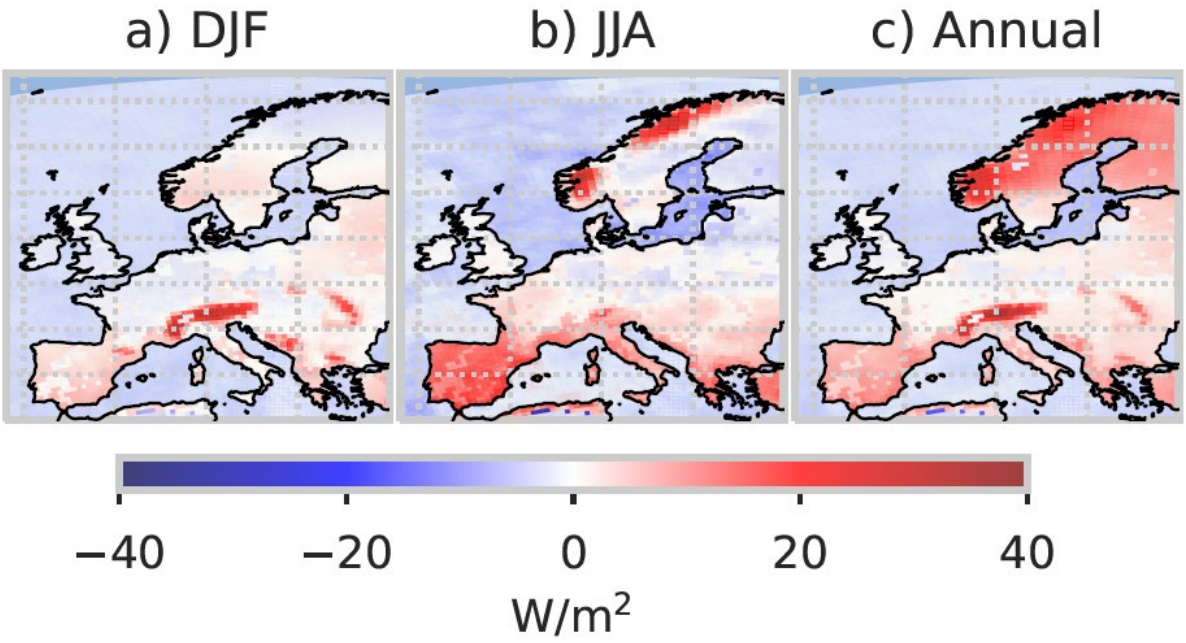

Figure 7: Changes in the TOA energy balance between CARBON and GRASS for (a) winter, (b) summer and (c) the whole year.

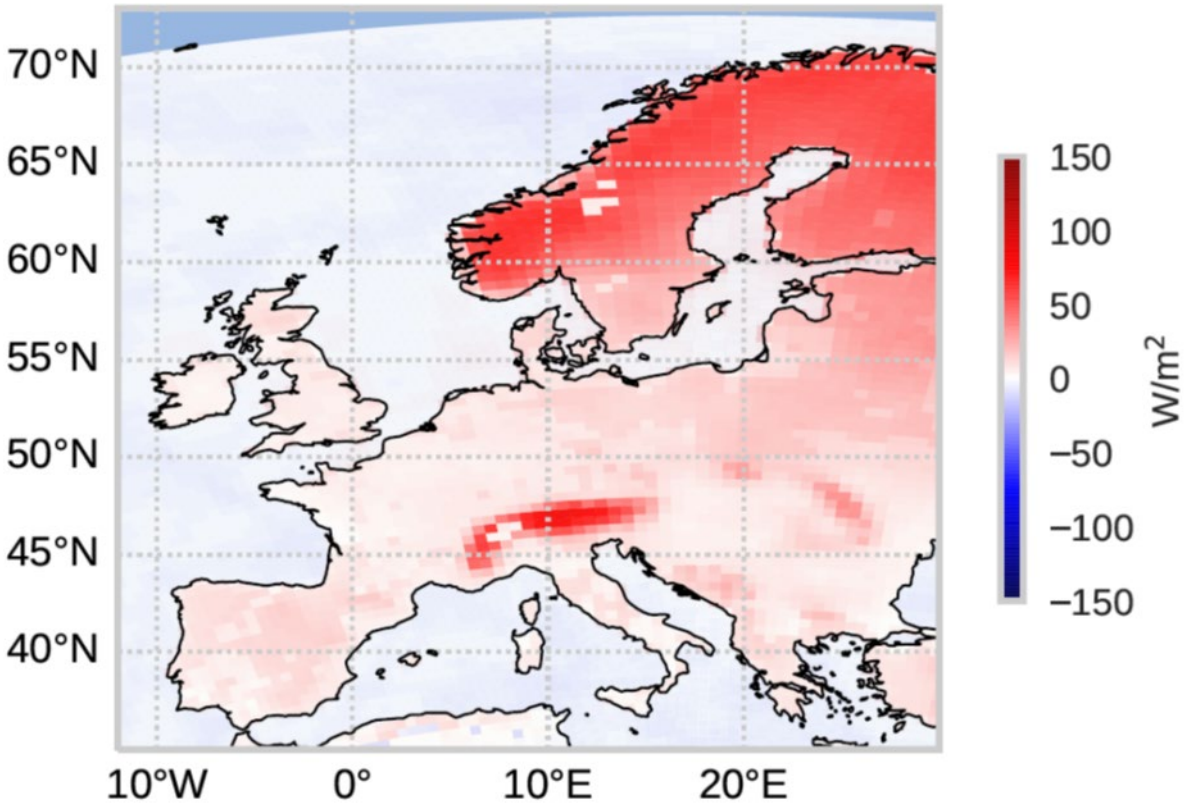

779

780 Figure 8: Mean differences in net shortwave radiation in spring between CARBON and GRASS for the

781 period 1986-2015.

782